J Dent Res 77(3):804-814, March, 1999

Contact Damage Resistance and Strength Degradation of Glass-infiltrated Alumina and Spinel Ceramics

Y.-G. Jung, I.M. Peterson, A. Pajares, and B.R. Lawn*

Materials Science and Engineering Laboratory, National Institute of Standards and Technology, Gaithersburg, Maryland 20899; *corresponding author

Abstract. All-ceramic crowns are coming into widespread use because of their superior esthetics and chemical inertness. This study examines the hypothesis that glass-infiltrated alumina and spinel core ceramics are resistant to damage accumulation and strength degradation under representative oral contact conditions. Accordingly, Hertzian indentation testing with hard spheres is used to evaluate damage accumulation in alumina and spinel ceramics with different pre-form grain morphologies and porosities. Indentation stress-strain curves measured on fully infiltrated materials reveal a marked insensitivity to the starting pre-form state. The glass phase is shown to play a vital role in providing mechanical rigidity and strength to the ceramic structures. All the infiltrated ceramics show subsurface cone fracture and *quasi*-plastic deformation above critical loads P_C (cracking) and P_Y (yield), depending on sphere radius, with $P_Y < P_C$. Strength degradation from accumulation of damage in Hertzian contacts above these critical loads is conspicuously small, suggesting that the infiltrated materials should be highly damage-tolerant to the "blunt" contacts encountered during mastication. Failure in the strength tests originates from either cone cracks ("brittle mode") or yield zones ("*quasi*-plastic mode"), with the brittle mode more dominant in the spinels and the *quasi*-plastic mode more dominant in the aluminas. Multi-cycle contacts at lower loads, but still above loads typical of oral function, are found to be innocuous up to 10^5 cycles in air and water, although contacts at 10^6 cycles in water do cause significant strength degradation. By contrast, contacts with Vickers indenters produce substantial strength losses at low loads, suggesting that the mechanical integrity of these materials may be compromised by inadvertent "sharp" contacts.

Key words: alumina, cracking, deformation, dental ceramics, Hertzian contact, microstructure, spinel, strength.

Received December 1, 1997; Last Revision April 2, 1998; Accepted June 8, 1998

Introduction

Glass-infiltrated ceramics are in clinical use as core materials in all-ceramic crowns and as inlays and onlays (Claus, 1990; Probster and Diehl, 1992; Probster, 1993; Hornberger, 1995; Rinke *et al.*, 1995; Seghi and Sorensen, 1995; Wolf, 1995; Giordano, 1996; Hornberger *et al.*, 1996; Wolf *et al.*, 1996; Kelly, 1997). The distinctive advantage of these ceramics is easy near-net-shape forming, yet high strength in the infiltrated state. However, these ceramics are subject to damage accumulation from repeated oral contact loading, even when covered by porcelain veneers. This disposition to contact damage is borne out by some reports of failures of all-ceramic crowns after a few years of use (Gindrat *et al.*, 1996; Kelly, 1997). It is therefore important to understand the damage and failure mechanisms in infiltrated ceramic materials under clinically relevant contact loading conditions in controlled laboratory settings. Accordingly, this study examines the hypothesis that multi-cycle contact fatigue in water does not cause significant strength degradation in glass-infiltrated alumina and spinel dental ceramics under representative oral loading conditions.

Of the available glass-infiltrated dental ceramics for use as core materials in crowns, alumina and spinel are the most widely used clinically. Alumina is the stronger of the two, while spinel is the more translucent (and may potentially be used without a veneer [Giordano, 1996]). These materials are supplied under the commercial name In-Ceram (Vita Zahnfabrik, Bad Sackingen, Germany)—as powders for slip-casting (alumina), and as dry-pressed partially sintered blocks for machining (alumina and spinel). Previous studies on alumina indicate that the microstructures of the slip-cast and dry-pressed materials are different: Whereas the microstructure in the slip-cast material is coarse and more heterogeneous, with platelike grains (Hornberger, 1995; Hornberger *et al.*, 1996), the dry-pressed material is finer and more homogeneous (Peterson *et al.*, 1998). In this context, it is useful to understand any effects of pre-form archi-

tecture and glass content on damage accumulation and ensuing strength degradation under contact loading conditions in the final restoration.

In this paper, we examine the contact damage and fatigue properties of glass-infiltrated alumina and spinel using the Hertzian contact test. The Hertzian test has been used previously for studying the responses of dental ceramics to contact damage (White *et al.*, 1995; Peterson *et al.*, 1998). Here, modes of damage from single-cycle and multi-cycle contact loading are identified, and data on strength degradation resulting from the accumulation of this damage are obtained. The damage modes are of two distinct types, traditional cone cracking ("brittle response") and distributed subsurface damage ("*quasi*-plastic response") (Lawn *et al.*, 1994). We conduct Hertzian tests on infiltrated materials with controlled microstructures: alumina, from slip-cast and dry-pressed preforms with different microstructures and different porosities; and spinels, from dry-pressed pre-forms with similar microstructures but different porosities. We explore the influence of microstructure on the mechanical responses in both the infiltrated and pre-form states, in the latter case to reinforce the crucial role of the subsequent glass infiltration in providing rigidity and resilience to dental restorations.

Materials and methods

Materials preparation and characterization

Specimens of alumina and magnesium-aluminate spinel were supplied by Vita Zahnfabrik (Bad Sackingen, Germany), in both pre-form and infiltrated states. (The mention of any commercial product in this paper does not imply endorsement by NIST.) The alumina pre-form structures were received in two forms, dry-pressed and slip-cast. The slip-cast alumina material (Vita In-Ceram®) is designed to be applied in layers onto a die and is sold commercially as a powder; the dry-pressed material (Vita Celay In-Ceram®) is designed to be machined from blanks into the shape of the restoration by means of the CELAY system (Kappert and Knode, 1993; Seghi and Sorensen, 1995; Giordano, 1996). The degrees of porosity of these two pre-forms were 20 vol% and 30 vol%, respectively (manufacturer's specifications). The pre-forms of spinel (Vita In-Ceram Spinell®) were also received in two forms, both dry-pressed but with different degrees of porosity, 12 vol% and 20 vol% (manufacturer's specifications). All the pre-forms for this study were machined into bars measuring 3 x 4 x 25 mm before infiltration by the supplier. Some uninfiltrated pre-form bars were set aside for comparison testing.

Most of the bars were infiltrated by the supplier with a La_2O_3-Al_2O_3-B_2O_3-SiO_2 glass (Vita In-Ceram A3.5®) by heat treatment for 80 min at 1100°C in the case of dry-pressed alumina, for 6 hrs at 1100°C in the case of slip-cast alumina, and for 20 min at 1130°C in the case of the spinels. After the bars cooled, the excess glass was removed by sandblasting. All specimens were ground to 10 μm finish on the top and bottom surfaces and were subsequently polished on the top surface to 1 μm in our laboratories. Selected polished surfaces were carbon-coated and examined in the scanning electron microscope so that the microstructures would be revealed.

For reference, some bulk glass specimens were prepared as disks 35 mm in diameter and 5 mm thick from the supplied glass powder by being heated to 1200°C in a gold-platinum crucible. After being air-cooled, these disks were given a second (annealing) heat treatment at 560°C for 1 hr. The surfaces of the disks were ground flat and polished, as described above.

Young's modulus was measured for the infiltrated structures and for the bulk glass infiltrate material by means of a routine pulse-echo sonic technique (McSkimin, 1961; Blessing, 1988). In this technique, an ultrasonic pulse is sent into the material, and the time interval between successive echoes is monitored by means of a transducer. Given the distance traveled by the signal during this time interval and the velocity of the signal, plus the density of the material (measured here by Archimedes' method), Young's modulus and Poisson's ratio can be calculated. In the present work, measurements were made on 5 specimens for each material.

We made Vickers diamond pyramid indentations on all materials to determine values of hardness (Tabor, 1951) and toughness (Anstis *et al.*, 1981) from measurements of plastic impression diagonals and radial crack lengths in conjunction with conventional indentation formulae. A minimum of 20 indentations was used on at least 4 specimens for each material over load ranges for which the hardness impressions and radial cracks were well-formed (from 5 to 10 N for hardness, and from 30 to 100 N for toughness).

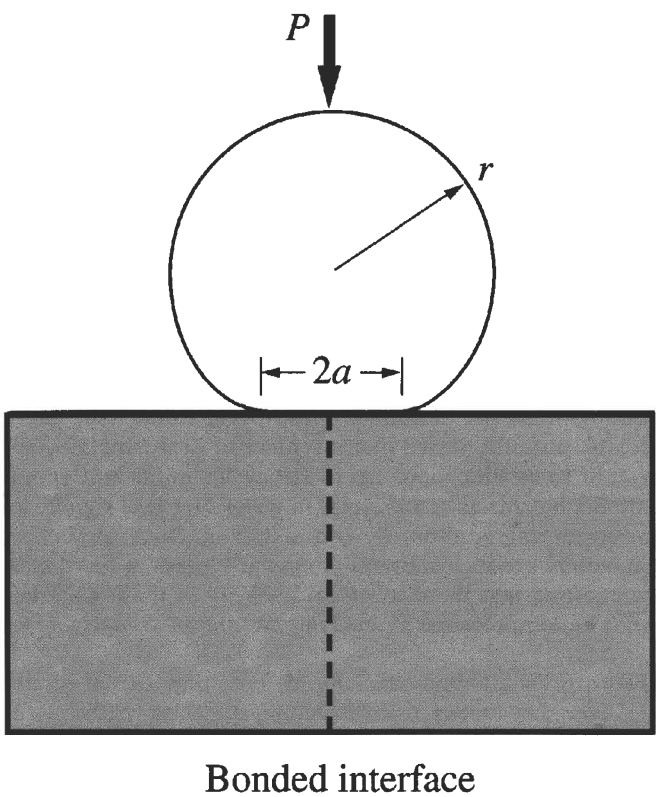

Figure 1. Schematic of Hertzian contact test, with sphere of radius r at load P over contact radius a. Specimen is pre-sectioned (vertical dashed line) to form "bonded-interface" specimen.

Contact damage and strength tests

Contact damage in the alumina and spinel specimens was introduced by means of the Hertzian test configuration shown in Fig. 1, with spherical tungsten carbide (WC) indenters. This test has been described in detail elsewhere (Guiberteau *et al.*, 1993; Peterson *et al.*, 1998), and only a brief description will be given here. All indentations in the contact experiments were made at crosshead speeds of 0.2 mm/min^{-1}, in air. We used hard WC spheres rather than a softer material similar in modulus to enamel, simply to avoid excessive deformation of the indenters, noting that softer indenters may still produce the same damage but at higher loads (Tabor, 1951).

Elastic–plastic responses of the aluminas and spinels were quantified by means of indentation stress-strain curves (Swain and Lawn, 1969; Guiberteau *et al.*, 1993; Cai *et al.*, 1994). Contact radii a were measured from residual traces on gold-coated specimen surfaces at prescribed loads P and sphere radii r, enabling plots of indentation stress, $p_0 = P/\pi a^2$, against indentation strain, a/r, to be calculated. Nonlinearity in such curves indicates the presence of *quasi*-plastic damage in the materials. In the present tests, a range of WC sphere sizes, r = 1.54–5.54 mm, was used to determine these curves. On these plots, each individual indentation produces a single point. A minimum of 20 indentations on 5 specimens was used to construct the curve for each material.

Surface and subsurface damage produced by the Hertzian contacts was observed by means of bonded-interface specimens (Mulhearn, 1959; Guiberteau *et al.*, 1994; Peterson *et al.*, 1998), in which two polished half-blocks were bonded together side-to-side with cyanoacrylate-based adhesive (Loctite Corp., Newington, CT) prior to indentation. Single-cycle indentations were made on the top surfaces of the specimens, with WC spheres of radius r = 3.18 mm at load P = 2500 N, in a row along the interface trace, spaced at least 4 mm apart. After completion of the indentations, the glue was dissolved in acetone to separate the surfaces. A thin coating of gold was applied to improve the contrast for qualitative identification of damage modes by optical microscopy in Nomarski interference.

Critical indentation loads for the onset of deformation, P_Y, and first cracking, P_C, were measured over a range of sphere radii r = 1.54–5.54 mm. These critical loads were determined visually from post-failure optical microscopy (Davies, 1949; Peterson *et al.*, 1998) by means of Nomarski interference contrast on the indented specimen surfaces—in these observations, a

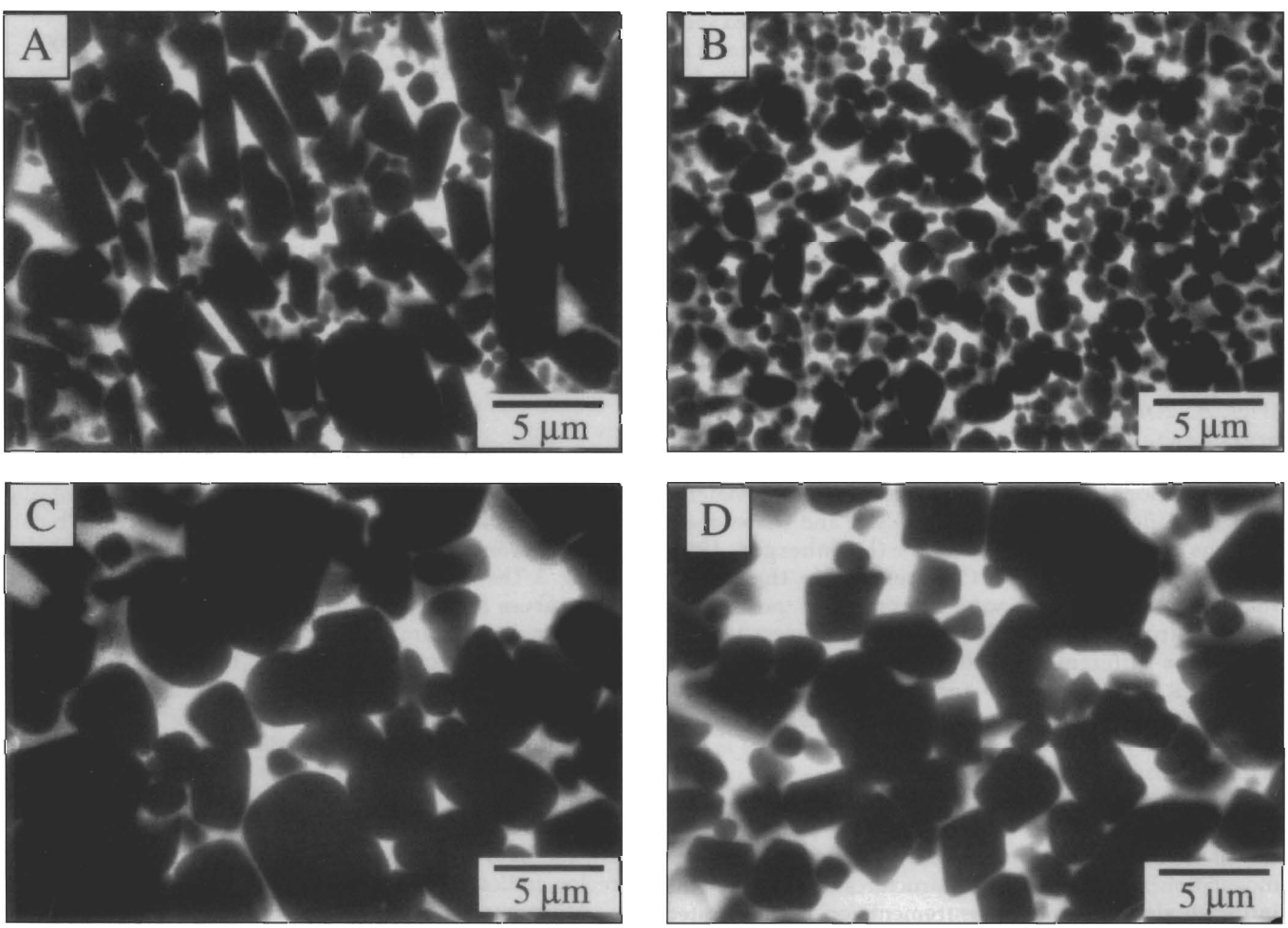

Figure 2. Scanning electron micrographs showing microstructures of glass-infiltrated In-Ceram materials: (A) alumina, slip-cast, 20 vol% glass; (B) alumina, dry-pressed, 30 vol% glass; (C) spinel, dry-pressed, 12 vol% glass; (D) spinel, dry-pressed, 20 vol% glass. As-polished surfaces, carbon-coated. Light phase is glass. Backscattered electron images.

post-contact gold coating was useful in enhancing image contrast. Means and uncertainty bounds for P_Y were determined from the load ranges over which the yield zones were both completely undetectable (lower limit) and clearly visible (upper limit). Analogous limits for P_C were determined from the load ranges over which the cone cracks first appeared on the surfaces as incipient shallow arcs and finally completed themselves as full surface rings around the contact. A minimum of 5 indentations at each ball size on each of 3 specimens was used to determine these limits.

Strength tests were conducted on bend bars after indentation with WC spheres of radius r = 3.18 mm. Single-cycle indentations were made at loads up to P = 2500 N, in air. Multi-cycle indentations were made at load P = 500 N for up to $n = 10^6$ cycles at frequency 10 Hz, in either air or water. In the slip-cast alumina, a few comparison tests were run on specimens indented with a Vickers diamond pyramid, at load P = 100 N. The indented specimens were then placed in a four-point bend fixture, inner span 10 mm and outer span 20 mm, with the indentations centrally located on the tensile side. A drop of silicone oil was placed onto each indentation site prior to bending, and the bending tests were conducted at a fast loading rate (500 mm/min^{-1}, fracture time < 40 ms), to minimize environmental effects in the strength data (Marshall and Lawn, 1980). (Surface tension maintains the oil within the cracks in the inverted specimens during bending.) Beam theory was used to determine the failure strengths from the breaking loads. Means and standard deviations for the strength values were obtained from an average of 5 breaks at each prescribed contact load.

Results

Materials characterization

Fig. 2 shows scanning electron micrographs of the infiltrated microstructures of alumina (Figs. 2A, 2B) and spinel (Figs. 2C, 2D). Dark areas indicate pre-form grains and light areas La_2O_3-Al_2O_3-B_2O_3-SiO_2 glass infiltrate. In the alumina, the grains in the slip-cast material (Fig. 2A) are larger and more elongate than those in the dry-pressed material (Fig. 2B), reflecting differences in the size and shape distributions of the starting powders (Hornberger, 1995; Hornberger *et al.*, 1996). (The texture in the former microstructure indicates some alignment of the alumina platelets from the pre-form slip-casting process.) In the spinel, the different glass contents reflect the pre-form porosities of 12% (Fig. 2C) and 20% (Fig. 2D). The dry-pressed spinel microstructures are geometrically similar to that of the dry-pressed alumina, though the spinel is substantially coarser.

Values of Young's modulus E measured by means of the pulse-echo technique are listed in the Table, along with values of hardness H and toughness T_0 (K_{IC}) from Vickers indentations, for the infiltrated structures and for the bulk infiltrate glass. Density measurements on the infiltrated materials indicate about 2 vol% residual porosity in the two aluminas and in the 20 vol% glass spinel material, and about 4 vol% residual porosity in the 12 vol% glass spinel.

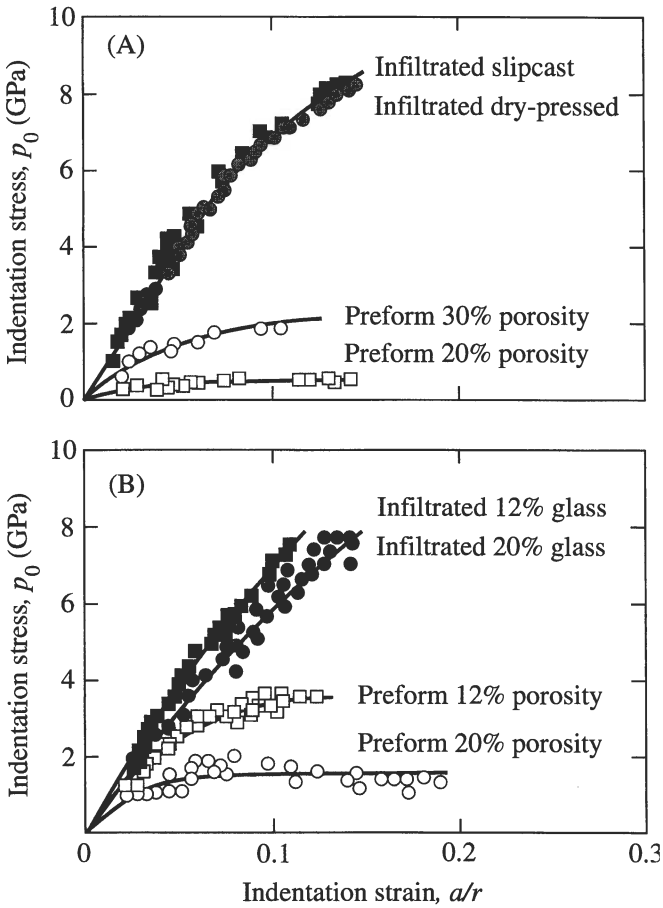

Figure 3. Indentation stress-strain curves: (A) alumina, slip-cast and dry-pressed; (B) spinel, dry-pressed. Data points represent individual indentations on 8-12 polished specimens of each material, in air, at a crosshead speed 0.2 min.min^{-1}. Filled circles are data for dense infiltrated state, open circles for porous preform state. Tests conducted using WC spheres, radii r = 1.54-5.54 mm (not distinguished).

Damage and strength properties

Indentation stress-strain data for the glass-infiltrated alumina and spinel structures (filled symbols), along with data for the corresponding pre-forms (open symbols), are shown in Fig. 3. The solid curves are empirical fits through the data. The curves for the pre-forms are strongly dependent on porosity, architecture, and degree of sintering—note that the pre-form with lower porosity is harder in the spinel, whereas the opposite is true in the alumina. On the other hand, the curves for the infiltrated structures are relatively insensitive to these factors. The data for the infiltrated aluminas (Fig. 3A) are slightly higher on the stress scale than those for the infiltrated spinels (Fig. 3B), consistent with slightly higher values of modulus and hardness in the Table. All the data show some non-linearity in the high-stress region, indicating the onset of "yield".

Micrographs from bonded-interface specimens show surface and subsurface damage patterns in the infiltrated structures, for contacts at r = 3.18 mm and P = 2500 N (Fig. 4): (A) infiltrated slip-cast alumina, (B) dry-pressed alumina, (C) 12

vol% glass spinel, and (D) 20 vol% glass spinel. These micrographs show well-developed *quasi*-plastic deformation and cone cracking. The largest of these cone cracks appear to be comparable in depth to the damage zones in the aluminas, but deeper in the spinels. Multiple cone cracks are visible in each material.

Critical loads for yield, P_Y, and for cone cracking, P_C, are plotted in Fig. 5 as a function of sphere radius r for all infiltrated materials. Both P_Y and P_C increase monotonically with r, indicating higher damage thresholds for "blunter" contacts. Note that these loads are insensitive to pre-form architecture or porosity. The values of P_Y are lower than those of P_C in all material systems, although the differences are substantially less in the spinel (Fig. 5B) than in the alumina (Fig. 5A). The relatively large load range for primary cone cracking (up to ± 25% of mean value) encompasses a prolonged evolutionary development in the crack geometry: initially as shallow, partial surface arcs; then as circumferential, shallow surface rings; and finally as fully developed cones. At higher loads, the surface traces of the primary cone cracks become engulfed within the expanding *quasi*-plastic compression–shear zone and close up, accounting for the initiations of secondary, shallower ring cracks of greater surface radii seen in Fig. 4 (Lawn *et al.*, 1998). The shaded areas in Fig. 5, labeled "oral zone", represent "typical" masticatory conditions (Peterson *et al.*, 1998). Note that in both material systems the P_Y and P_C data lie above these oral zones over most of the data range—intersections with this zone occur only at very small r, and only with the P_Y data.

Strengths of the glass-infiltrated alumina and spinel materials are shown as a function of Hertzian contact load in Fig. 6, after indentation at r = 3.18 mm, in air. In these plots, the data points are experimental results, and the solid curves are empirical fits through the data. Filled circles represent failures from indentation damage sites: in the alumina, fracture originates from either cone cracks or *quasi*-plastic zones, in the manner shown in Fig. 7; in the spinel, fracture originates almost exclusively from cone cracks. Open circles in Fig. 6 represent failures from natural flaws in indented specimens. Open boxes at the strength axes represent failures from natural flaws in unindented (as-polished) infiltrated specimens. Lower shaded boxes on these same axes represent failures from natural flaws in unindented porous pre-forms—clearly, the infiltration greatly strengthens the structures. Shaded boxes on the load axes indicate the ranges of P_Y and P_C for r = 3.18 mm (from Fig. 5). The strength data show a very modest decline in strength above the onset of contact damage in all four materials, out to high loads, P > 2500 N. Note the higher post-damage strengths of the aluminas in comparison with the spinels, consistent with the higher toughness values in the Table.

Results of a contact fatigue case study on slip-cast alumina are shown in Fig. 8 for indentations at load P = 500 N and r = 3.18 mm in water. In this case study, the slip-cast alumina is chosen because of its relative susceptibility to *quasi*-plasticity, the load P = 500 N because it lies just above P_Y for yield (but well below P_C for cracking) (Fig. 5), and water because it represents a highly deleterious environment. In Fig. 8A, strengths are plotted as a function of number of cycles. These strengths remain unaffected up to n = 10^5 cycles, but fall off precipitously at n = 10^6. The indented surface, relatively featureless up to n = 10^5, shows signs of surface "fretting" damage after 10^6 cycles in water (Fig. 8B). Examination of the specimens after strength testing indicates breaks from natural flaws up to n = 10^5 (open symbols); at n = 10^6, breaks occur from the damage zone with the same failure pattern as Fig. 7b, indicating the build-up of strength-degrading subsurface *quasi*-plasticity.

The bar chart of Fig. 9 compares strength data for the infiltrated alumina and spinel materials, for unindented (as-polished) and indented (r = 3.18 mm, P = 500 N) states, and for single-cycle and multi-cycle contacts. For each material group, the bar sequence is as follows: a, as-polished, unindented; b, single-cycle indentations, in air; c, multi-cycle indentations, n = 10^5, in water; and d, multi-cycle indentations, n = 10^6, in water. In all materials, fractographic observations confirm failures from natural flaws in the states a–c, and from indentation sites, specifically *quasi*-plastic zones, in state d. ANOVA and Neuman Keuls Multiple Comparisons tests show no significant differences (p > 0.05) among states a–c within each material group, indicating a high degree of damage tolerance in these materials. Strength reductions for the state d at 10^6 cycles in water relative to states a–c are significant for the first three material groups (p < 0.05), but not for the 20 vol% spinel (p > 0.05).

Comparisons between the strengths of the four materials across all test conditions found no significant strength differences between the infiltrated slip-cast and dry–pressed aluminas, or between the infiltrated spinels (p > 0.05). On the other hand, the difference in strengths of the two spinels relative to the two aluminas in Fig. 9 is significant (p < 0.0001).

A comparison set of strength tests on slip-cast alumina after Vickers indentation at a relatively low single-cycle load P = 100 N shows a much greater drop in strength, to 199 ± 38 MPa (*cf.* 430 ± 26 MPa for Hertzian indentation at P = 2500 N, Fig. 6), characteristic of a more brittle response. This simple result indicates that the damage tolerance implied above for single-cycle blunt contacts does not extend to extreme sharp contacts.

Table. Material parameters (means ± standard deviations) for glass-infiltrated alumina and spinel ceramics

Material	Pre-form	Glass Content (vol %)	Young's Modulus E (GPa)	Hardness[a] H (GPa)	Toughness[a] T_0 (MPa.m$^{1/2}$)
Alumina	slip-cast	20	271 ± 9	12.3 ± 0.5	2.89 ± 0.2
Alumina	dry-pressed	30	254 ± 4	11.8 ± 0.4	2.46 ± 0.2
Spinel	dry-pressed	12	212 ± 7	11.6 ± 0.4	1.79 ± 0.2
Spinel	dry-pressed	20	203 ± 3	10.8 ± 0.4	1.88 ± 0.2
Glass	infiltrate	—	101 ± 3	7.1 ± 0.2	0.9 ± 0.1

[a] Measured over Vickers load range 5-10 N for hardness, and 30-100 N for toughness.

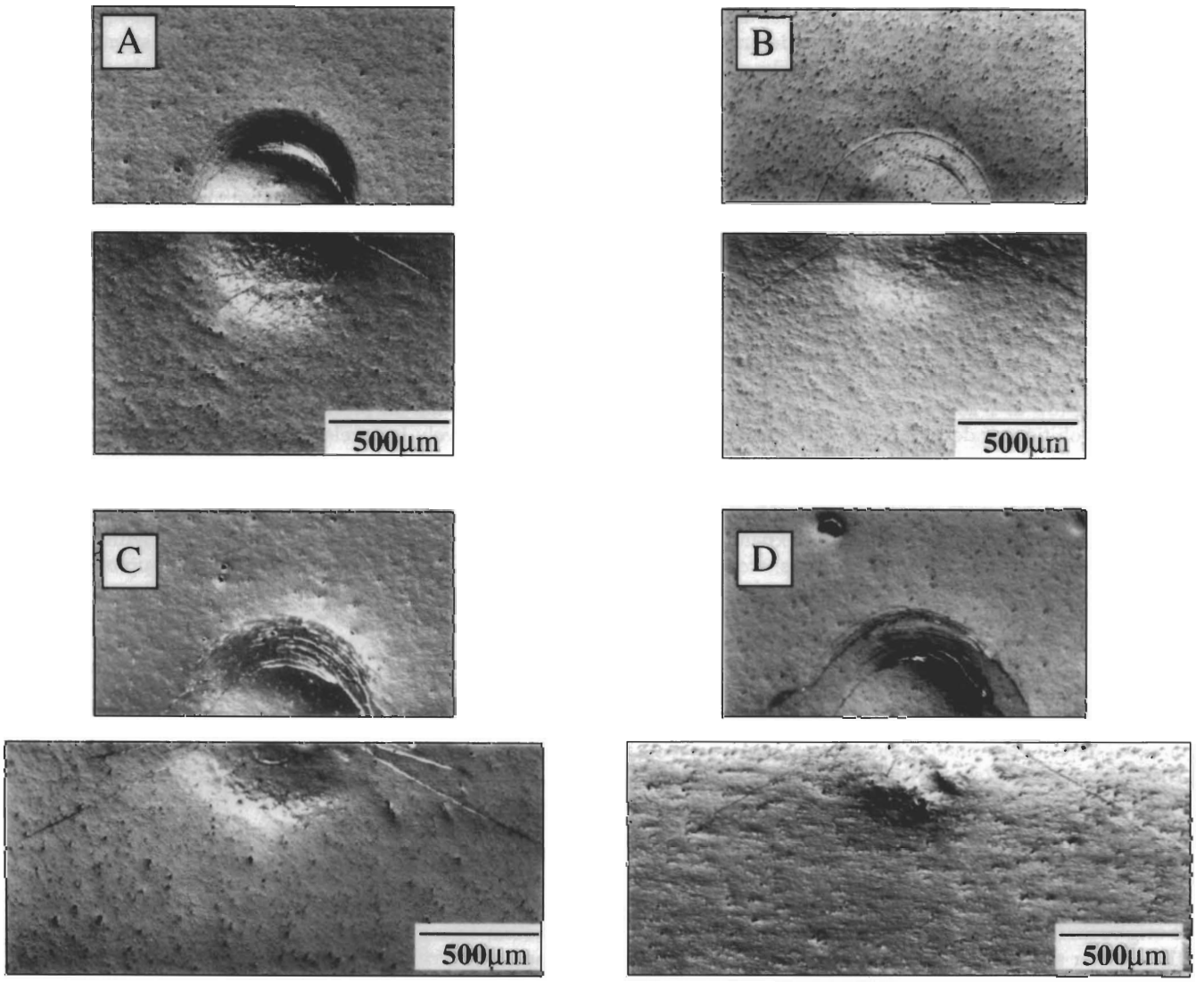

Figure 4. Half-surface (upper) and section (lower) views of Hertzian contact damage, for glass-infiltrated materials: (A) alumina, slip-cast, 20 vol% glass; (B) alumina, dry-pressed, 30 vol% glass; (C) spinel, dry-pressed, 12 vol% glass; (D) spinel, dry-pressed, 20 vol% glass. Indentations with a WC sphere, r = 3.18 mm, P = 2500 N. Traces of both cone cracking and *quasi*-plasticity are observed. Bonded-interface specimens, Nomarski optical micrographs.

Discussion

We have demonstrated that glass-infiltrated alumina and spinel dental ceramics are subject to damage accumulation in high-load contacts. We identify two distinct modes of damage (Fig. 4), cone cracking (brittle mode) and yield deformation (*quasi*-plastic mode). In their well-developed states, these two competing damage types appear to be of comparable scales. However, the critical load for yield, P_Y, is considerably lower than that for cracking, P_C, over a wide range of indenter radii (Fig. 5), especially in the aluminas. These results imply a class of forgiving ceramic materials that are able to absorb a substantial portion of the contact strain energy in *quasi*-plastic deformation rather than in fracture, and that are less susceptible to catastrophic failure than traditional brittle materials like glasses, porcelains, and other fine-grain ceramics.

The stress-strain data for the pre-form and infiltrated alumina and spinel materials (Fig. 3) provide some instructive intra-comparisons. The key finding in these data is the relative insensitivity of the responses of the infiltrated materials to the starting pre-form microstructures. This insensitivity extends to the critical loads for yield and cracking (Fig. 5). On the other hand, the comparative stress–strain curves for the pre-forms in Fig. 3 lie well below those for the corresponding infiltrated materials, indicating that porosity (as well as architecture—recall the inversion of the 30% and 20% data in Fig. 3A) can be a vital factor in performance. This indication is consistent with previous observations of greatly enhanced *quasi*-plasticity in porous alumina ceramics, in which deformation may accumulate rapidly from pore collapse or enhanced microcracking (Latella *et al.*, 1997). The implication is that the

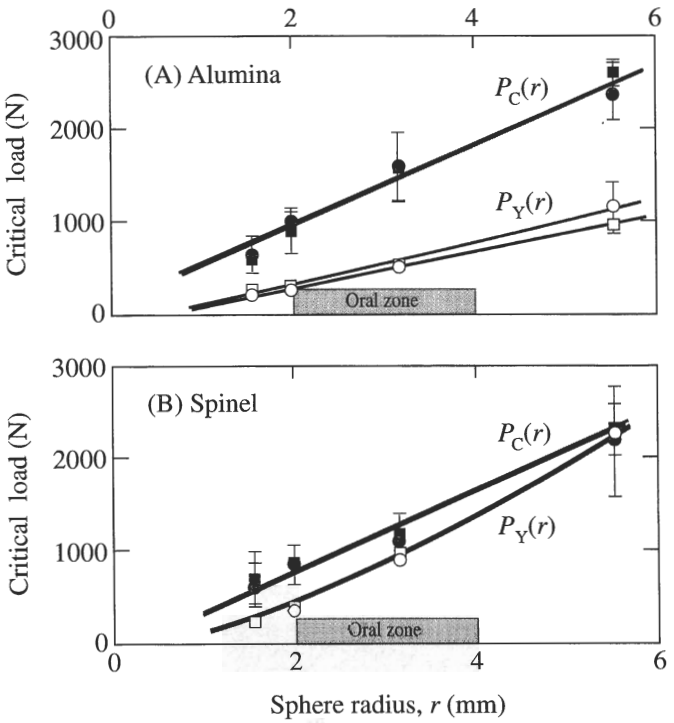

Figure 5. Critical loads for onset of subsurface yield (P_Y) and surface cracking (P_C) as function of WC sphere radius (r): (A) alumina, slip-cast (squares) and dry-pressed (circles); (B) spinel, dry-pressed, 12 vol% glass (squares) and 20 vol% glass (circles). Open symbols indicate porous pre-forms, closed symbols infiltrated structures. Shaded zones indicate "typical" range of oral masticatory conditions. Each point represents a minimum of five indentations. Error bars are uncertainty bounds. (For the P_Y values, the uncertainty levels are less than ± 25 N, too small to register on the graph.) Note that critical load for yield is lower than that for cracking over the bulk of the radius range in all cases.

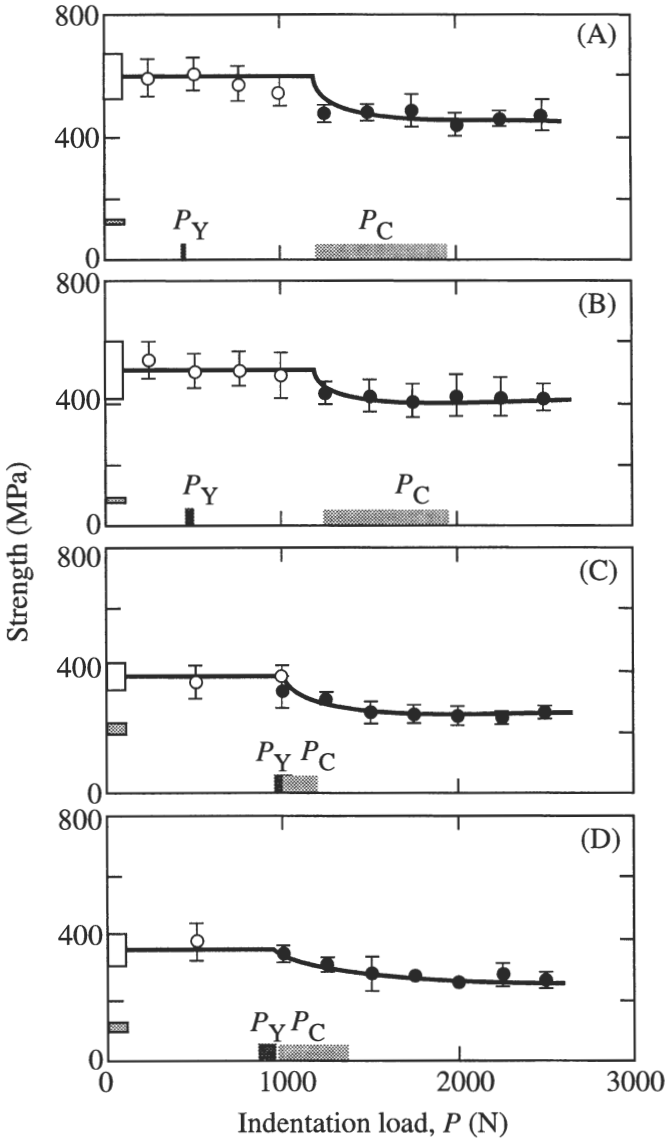

Figure 6. Strength of glass-infiltrated materials after indentation with WC sphere, r = 3.18 mm, as function of contact load: (A) alumina, slip-cast, 20 vol% glass; (B) alumina, dry-pressed, 30 vol% glass; (C) spinel, dry-pressed, 12 vol% glass; (D) spinel, dry-pressed, 20 vol% glass. Data are means and standard deviations of a minimum of 5 specimens at each load—closed symbols represent failures from indentation origins, open symbols from other origins. Open box at left axis represents strengths of polished, unindented specimens; shaded box represents strengths of porous pre-forms. Ranges of critical loads P_Y and P_C indicated at horizontal axis (from Fig. 5).

properties of the alumina and spinel materials are not highly dependent on the processing route, provided the glass infiltration is essentially complete (recall the porosities 2–4% in our infiltrated materials).

Some caution needs to be exercised when using the bonded-interface technique to evaluate the extent of damage. As previously pointed out (Peterson *et al.*, 1998), comparisons with polished sections made *after* indentation indicate that the damage configurations are qualitatively representative of those in bulk specimens, but that absolute dimensions of the damage types can be affected by the presence of the soft adhesive interface between the two half-specimens. Specifically, the sizes of the cone cracks on the separated faces can be exaggerated relative to the true values in a bulk specimen. These crack sizes may also be enhanced by residual stresses associated with the *quasi*-plastic zones—such stresses are known to continue to drive existing cracks, and even to create new cracks, well after indentation is complete, especially in the vicinity of free surfaces (Lawn *et al.*, 1985; Padture, 1993). (For this reason, it is desirable to keep the adhesive layer as thin as possible, preferably < 10 μm.) Accordingly, the bonded-interface specimen should not be regarded as a reliable source of *quant*itative analysis. Nevertheless, as a *qual*itative tool for observing the form of the damage modes, particularly the *quasi*-plasticity modes, the bonded-interface provides much more striking visible information than conventional polished sections.

Strength degradation associated with damage from single-cycle "blunt" Hertzian contacts occurs at high loads (P > 1000 N for indenters of radius r = 3.18 mm, Fig. 6) in all the infiltrated materials studied here. The strength losses in this

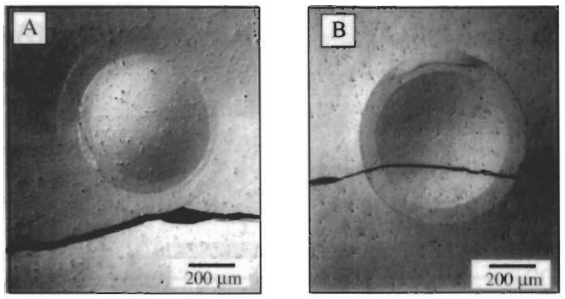

Figure 7. Failure origins in dry-pressed In-Ceram alumina after indentation with WC sphere at P = 2500 N, r = 3.18 mm: (A) origin at surface ring crack; (B) origin inside, *quasi*-plastic deformation zone. Nomarski optical micrographs.

high-load region are associated with failures from either cone cracks or *quasi*-plastic zones in the alumina (Fig. 7), predominantly from cone cracks in the spinel. However, these losses are modest, unlike the abrupt falloffs at $P = P_C$ that typify traditional failures from cone cracks (Lawn *et al.*, 1975, in press) and more like the gradual losses that characterize failures from *quasi*-plastic zones (Lawn *et al.*, 1998; Lee and Lawn, in press; Peterson *et al.*, 1998). The fact that, in the aluminas, the failures mostly initiate from *quasi*-plastic zones instead of from cone cracks not only confirms that the *quasi*-plastic zones are themselves far from benign but also suggests that these same *quasi*-plastic zones interact with the cone cracks to neutralize the latter's effectiveness. The fact that the ring cracks form gradually into the full cone configuration over a broad spread of indentation loads (Figs. 5, 6), instead of spontaneously and abruptly from an initially invisible surface flaw at a well-defined critical load, suggests a strong moderating influence of the *quasi*-plasticity on the fracture mode.

For slip-cast alumina specimens containing "sharp" Vickers indentations at relatively low load (P = 100 N), the strength loss is much more substantial (down to 199 ± 38 MPa, relative to 430 ± 26 MPa for Hertzian indentations at P = 2500 N, Fig. 6). Thus, concentrated sharp contacts, which traditionally produce more deleterious (radial) cracks at much lower loads (Lawn and Wilshaw, 1975; Lawn *et al.*, 1976), could negate any damage tolerance.

From the standpoint of clinical relevance, the results presented in this study suggest that glass-infiltrated alumina and spinel ceramics are not highly susceptible to damage, at least for Hertzian contacts within the typical cuspal radius range, 2–4 mm (Wheeler, 1958), and normal mastication loads up to 200 N (DeLong and Douglas, 1983; Anusavice, 1989; Phillips, 1991; Craig, 1997) (oral zones, Fig. 5). Even the clear presence of well-developed cone cracks above critical initiation loads or above a critical number of cycles may not catastrophically diminish the strength of a damaged restoration (Fig. 4). On the other hand, the inadvertent contact with a sharp particle during chewing, even at loads well below the maximum in mastication, carries a real threat of introducing fatal flaws that could lead to premature failure. This enhanced susceptibility to sharp contacts is most pertinent to restorations that have direct access to

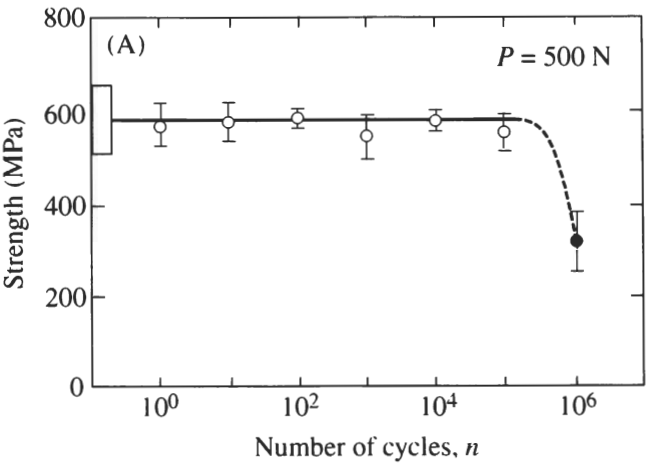

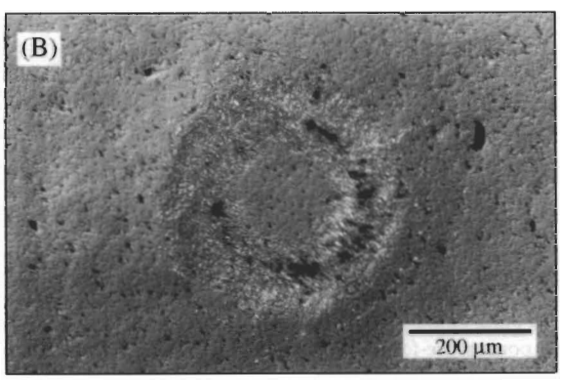

Figure 8. (A) Strength of glass-infiltrated slip-cast alumina after indentation with WC sphere, r =3.18 mm and P = 500 N, in water, as function of number of cycles n. Data are means and standard deviations of a minimum of 5 specimens at each number of cycles n—closed symbols represent failures from indentation origins, open symbols from other origins. Open box at left axis represents strengths of polished, unindented specimens. (B) Surface view of contact damage in slip-cast alumina specimen after $n = 10^6$ cycles. Note surface fretting. Nomarski optical micrograph.

the chewing environment, as with inlays and onlays. When the materials are used as core materials for crowns, porcelain veneers afford partial protection—there, the strength of the underlying core is threatened only by imperfect finishing of the initial restoration (*e.g.*, from machining or sandblasting flaws (Peterson *et al.*, in press)). In that case, the limiting factor becomes the strength of the porcelain veneer, or of the veneer/core interface.

A key factor in the oral environment is the presence of water. Water is notorious as a deleterious environment in crack growth (Wiederhorn, 1967) and diffuse damage accumulation (Guiberteau *et al.*, 1993) in ceramics. In Fig. 8A, the influence of water on the contact process is demonstrated in multi-cycle contact tests at a load level well below P_C but just above P_Y (P = 500 N, r = 3.18 mm—*cf.* Fig. 5). In those tests, no significant strength degradation is observed until a critical number of cycles is attained ($n = 10^6$). In the critical region, superficial surface fretting (Fig. 8B), attributable to frictional sliding at asperities between indenter and speci-

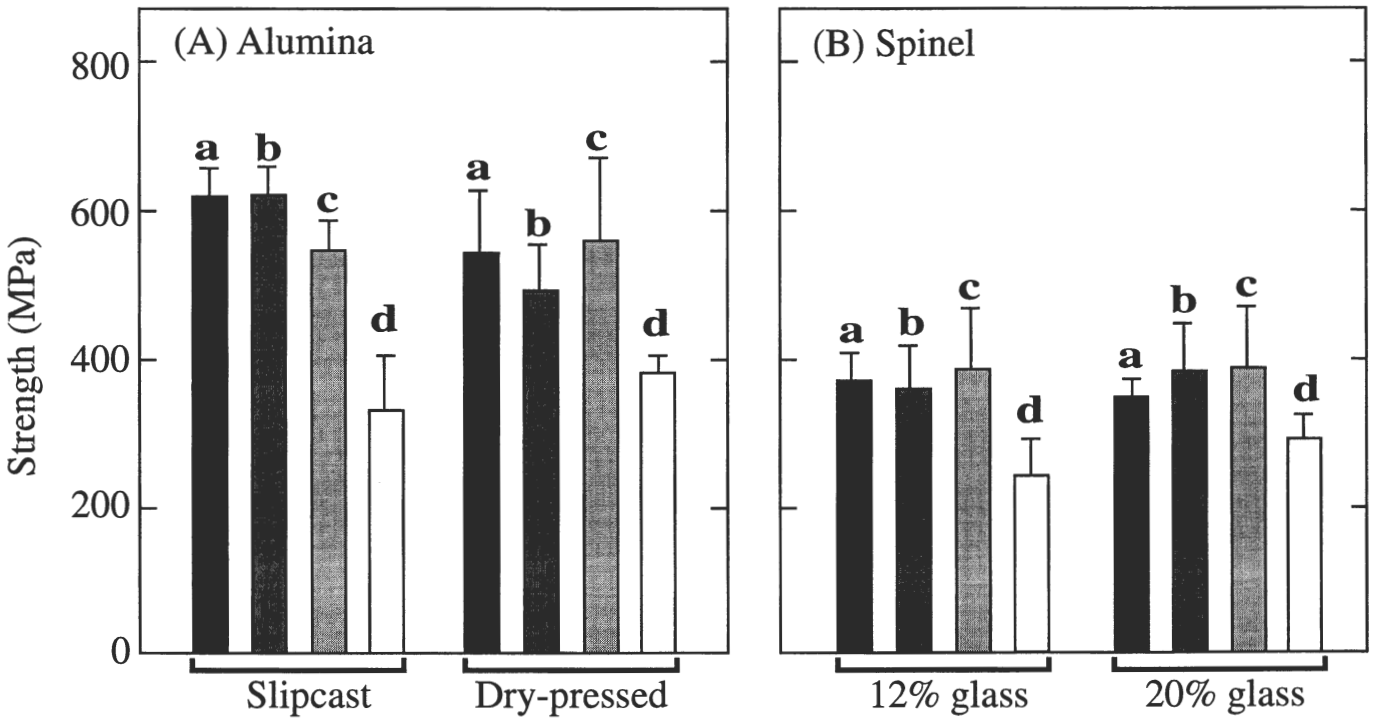

Figure 9. Strengths of infiltrated In-Ceram, indentations at r = 3.18 mm and P = 500 N: (A) alumina, slip-cast and dry-pressed; and (B) spinel, 12 vol% and 20 vol% glass. Strength sequence: a, unindented. control (as-polished); b, single-cycle indent in air; c, multi-cycle indent, $n = 10^5$, in water; and d, multi-cycle indent, $n = 10^6$, in water. Error bars are standard deviations, minimum of 5 specimens.

men in an annular contact region (Johnson, 1985), somewhat obscures the true strength-degrading damage—subsurface *quasi*-plasticity in the slip-cast alumina and incipient surface ring cracking in the other materials. (While not usually deleterious to strength, the fretting damage may nevertheless be highly pertinent to wear properties [Kennedy *et al.*, 1994].) Such tests indicate that the values of P_C and P_Y measured in ordinary atmospheres (*e.g.*, Fig. 5) can be substantially diminished by chemical interactions. Earlier single-cycle Hertzian studies on soda-lime glass have demonstrated that the values of P_C for cone fracture may be diminished by more than a factor of three by prolonged exposures to water under sustained loads (Langitan and Lawn, 1970). Nevertheless, the P_C values for the glass-infiltrated materials studied here lie so far above the oral zone in Fig. 5 that water is unlikely to diminish the fracture thresholds sufficiently to pose the threat of brittle failure. On the other hand, the values of P_Y lie much closer to the oral zone, so that water-induced chemical effects may well be a crucial issue in the accelerated development of *quasi*-plasticity (Guiberteau *et al.*, 1993). In this context, recall that the failure at $n = 10^6$ cycles in Fig. 8 indeed occurred in the *quasi*-plastic mode. The micromechanics of chemically enhanced *quasi*-plasticity in dental ceramics requires further study.

As indicated in the "Experimental" section, hard WC spheres rather than lower modulus spheres more representative of tooth enamel were used in the present Hertzian tests. The use of WC spheres simply preserves the lifetime of the indenters. This choice of indenter material should not be seen as a limitation, because even soft indenters can create the same kind of contact damage in harder materials, albeit at higher loads. This is because the indentation pressures continue to rise well beyond the point of first yield in monotonic loading, so even a yielding indenter can ultimately generate high contact stresses (Tabor, 1951; Peterson *et al.*, 1998). Testing with harder spheres would appear to place a lower bound on performance. On the other hand, the tests in the present study were conducted in purely normal loading, without the attendant sliding, spurious sharp contacts, or other deleterious conditions representative of actual mastication that might enhance failure of restorations. In this context, the Hertzian test should be viewed as an ideally simple tool for evaluating and screening prospective dental materials, rather than as a strict simulator of actual dental function.

From a materials processing standpoint, we have shown that the indentation stress-strain responses (Fig. 3), critical loads for the onset of damage (Fig. 5), and strengths of infiltrated materials after damage (Fig. 6) are somewhat insensitive to material pre-form architecture (again, provided the infiltration is complete). Thus, the infiltration processing route is very "forgiving", and not as critically dependent on the skills of the dental technician, consistent with the relatively high survival rates of molar crowns prepared by this technology, at least in the short term (Probster, 1993, 1996). The pre-form architecture itself may then be chosen on the basis of other factors (*e.g.*, ease of processing, machinability), without compromising ultimate clinical lifetime.

Acknowledgments

The authors thank S. Wuttiphan, M.B. Bush, S.K. Lee, H. Chai, V.P. Thompson, and J.R. Kelly for many fruitful discussions. E. Romberg performed the statistical analysis. G.V. Blessing and J.A. Slotwinski assisted in obtaining the elastic modulus values. D.H. Blackburn prepared the bulk glass specimens. This work was funded under NIDR Grant PO1 DE10976.

References

Anstis GR, Chantikul P, Marshall DB, Lawn BR (1981). A critical evaluation of indentation techniques for measuring fracture toughness: I. Direct crack measurements. *J Am Ceram Soc* 64:533-538.

Anusavice KJ (1989). Criteria for selection of restorative materials: properties vs technique sensitivity. In: Quality evaluations of dental restorations. Anusavice KJ, editor. Chicago: Quintessence, pp. 15-56.

Blessing GV (1988). The pulsed ultrasonic velocity method for determining material dynamic elastic moduli. In: Symposium on dynamic modulus measurements, Wolfenden A, editor. Kansas City, MO: ASTM, pp. 47-57.

Cai H, Stevens Kalceff MA, Lawn BR (1994). Deformation and fracture of mica-containing glass–ceramics in Hertzian contacts. *J Mater Res* 9:762-770.

Claus H (1990). Vita InCeram, a new system for producing aluminum oxide crown and bridge substructures. *Quintessenz Zahntech* 16:35-46.

Craig RG (1997). Mechanical properties. In: Restorative dental materials. Chapter 4. Craig RG, editor. St. Louis: Mosby.

Davies RM (1949). Determination of static and dynamic yield stresses using a steel ball. *Proc R Soc Lond* 197(A):416-432.

DeLong R, Douglas WH (1983). Development of an artificial oral environment for the testing of dental restoratives: biaxial force and movement control. *J Dent Res* 62:32-36.

Gindrat P, Scherrer SS, de Rijk WG, Belser UC (1996). Lifetime determination of InCeram restorations from censored clinical data (abstract). *J Dent Res* 75(Spec Iss):249.

Giordano RA (1996). Dental ceramic restorative systems. *Compend Contin Educ Dent* 17:779-794.

Guiberteau F, Padture NP, Cai H, Lawn BR (1993). Indentation fatigue: a simple cyclic Hertzian test for measuring damage accumulation in polycrystalline ceramics. *Phil Mag* 68(A):1003-1016.

Guiberteau F, Padture NP, Lawn BR (1994). Effect of grain size on Hertzian contact in alumina. *J Am Ceram Soc* 77:1825-1831.

Hornberger H (1995). Strength microstructure relationships in a dental alumina glass composite (PhD dissertation). University of Birmingham, UK.

Hornberger H, Marquis PM, Christiansen S, Strunk HP (1996). Microstructure of a high strength alumina glass composite. *J Mater Res* 11:855-858.

Johnson KL (1985). Contact mechanics. Chapter 7. London: Cambridge University Press.

Kappert H, Knode H (1993). InCeram: testing a new ceramic material. *Quintessence Dent Technol* 16:87-97.

Kelly JR (1997). Ceramics in restorative and prosthetic dentistry. *Ann Rev Mater Sci* 27:443-468.

Kennedy PJ, Conte AA, Whitenton EP, Ives LK, Peterson MB (1994). Surface damage and mechanics of fretting wear in ceramics. In: Friction and wear of ceramics. Jahanmir S, editor. New York: Marcel Dekker, pp. 79-98.

Langitan FB, Lawn BR (1970). Effect of a reactive environment on the Hertzian strength of brittle solids. *J Appl Phys* 41:3357-3365.

Latella BA, O'Connor BH, Padture NP, Lawn BR (1997). Hertzian contact damage in porous alumina ceramics. *J Am Ceram Soc* 80:1027-1031.

Lawn BR, Wilshaw TR (1975). Indentation fracture: principles and applications. *J Mater Sci* 10:1049-1081.

Lawn BR, Wiederhorn SM, Johnson H (1975). Strength degradation of brittle surfaces: blunt indenters. *J Am Ceram Soc* 58:428-432.

Lawn BR, Fuller ER, Wiederhorn SM (1976). Strength degradation of brittle surfaces: sharp indenters. *J Am Ceram Soc* 59:193-197.

Lawn BR, Jakus K, Gonzalez AC (1985). Sharp vs blunt crack hypotheses in the strength of glass: a critical study using indentation flaws. *J Am Ceram Soc* 68:25-34.

Lawn BR, Padture NP, Cai H, Guiberteau F (1994). Making ceramics "ductile". *Science* 263:1114-1116.

Lawn BR, Lee SK, Peterson IM, Wuttiphan S (1998). A model of strength degradation from Hertzian contact damage in tough ceramics. *J Am Ceram Soc* 81:1509-1520.

Lee SK, Lawn BR (1998). Role of microstructure in Hertzian contact damage in silicon nitride: II. Strength degradation. *J Am Ceram Soc* 81:997-1003.

Marshall DB, Lawn BR (1980). Flaw characteristics in dynamic fatigue: the influence of residual contact stresses. *J Am Ceram Soc* 63:532-536.

McSkimin HJ (1961). Pulse-superposition methods for measuring ulatrasonic wave velocities in solids. *J Acoust Soc Am* 33:12-16.

Mulhearn TO (1959). The deformation of metals by Vickers-type pyramidal indenters. *J Mech Phys Solids* 7:85-96.

Padture NP (1993). Postfailure subsidiary cracking from indentation flaws. *J Mater Res* 8:1411-1417.

Peterson IM, Pajares A, Lawn BR, Thompson VP, Rekow ED (1998). Mechanical characterization of dental ceramics using Hertzian contacts. *J Dent Res* 77:589-602.

Phillips RW (1991). Skinner's science of dental materials. Philadelphia: W.B. Saunders.

Probster L (1993). Survival rate of In-Ceram restorations. *Int J Prosthodont* 6:259-263.

Probster L (1996). Four year clinical study of glass-infiltrated, sintered alumina crowns. *J Oral Rehabil* 23:147-151.

Probster L, Diehl J (1992). Slip casting alumina ceramics for crown and bridge restorations. *Quintessence Int* 23:25-31.

Rinke S, Huls A, Jahn L (1995). Marginal accuracy and fracture strength of conventional and copy-milled all-ceramic crowns. *Int J Prosthodont* 8:303-310.

Seghi RR, Sorensen JA (1995). Relative flexural strength of six new ceramic materials. *Int J Prosthodont* 8:239-246.

Swain MV, Lawn BR (1969). A study of dislocation arrays at spherical indentations in LiF as a function of indentation stress and strain. *Phys Stat Sol* 35:909-923.

Tabor D (1951). Hardness of metals. Oxford: Clarendon.

Wheeler RC (1958). A textbook of dental anatomy and physiology. Philadelphia, PA: W.B. Saunders.

White SN, Zhao XY, Zhaokun Y, Li ZC (1995). Cyclic mechanical fatigue of a feldspathic dental porcelain. *Int J Prosthodont* 8:413-420.

Wiederhorn SM (1967). Influence of water vapor on crack propagation in soda-lime glass. *J Am Ceram Soc* 50:407-414.

Wolf WD (1995). Strength and fracture toughness of alumina-glass dental composites prepared by melt-infiltration (PhD dissertation). Minneapolis: University of Minnesota.

Wolf WD, Vaidya KJ, Francis LF (1996). Mechanical properties and failure analysis of alumina-glass dental composites. *J Am Ceram Soc* 79:1769-1776.